3. Results

The median duration of lower body circulatory arrest, SCP, CPB, and surgery were 68, 147, 209, and 415 min, respectively. The median transfusion volume was 2400 ml. There were three hospital deaths (2.5%) from perioperative myocardial infarction, low cardiac output with bowel necrosis, and mediastinitis. Two patients (1.7%) developed permanent neurological dysfunction (small stroke), and three patients (2.5%) suffered from transient cerebral deficits. Three patients (2.5%) required reentry for bleeding. In none of them, bleeding from the distal anastomosis was found. Other complications occurred: low cardiac output in 5.0%, respiratory failure in 10.0%, renal failure in 3.3%, hepatic failure in 0.8%, bowel necrosis in 1.7%, and sepsis in 0.8%.

4. Discussion

The most common approach for arch to distal arch aneurysms is currently through median sternotomy [1–4]. This approach aims to provide cerebral and cardiac safety. However, the distal anastomosis tends to be difficult because of poor, distant, and limited view [6,7]. In our technique, the arch aneurysm is not incised to prevent injury to the nerves and lung. Through the aneurysm, the descending aorta is divided and the distal anastomosis takes place. Subsequently, the surgical view is limited. Furthermore, bleeding from this anastomosis is a major concern. We have therefore evolved a novel stepwise technique, which made the distal anastomosis around the hilum feasible in our experience.

The end of the descending aorta is often fragile with much atherosclerosis. Even with the stepwise technique, we experienced bleeding from the anastomosis in seven patients. The stepwise technique was therefore refined by the "mini-elephant trunk". With this refinement, we have not experienced any major bleeding from the distal anastomosis.

The stepwise technique has some drawbacks. Graft insertion carries a risk of dislodging mural atheroma. We experienced one case of bowel necrosis. To prevent this problem, in the refined technique, the distal end was tucked inside to shorten the graft length. Graft insertion must be done carefully into the atheromatous descending aorta. Direct anastomosis of a short-length graft without graft insertion is a good alternative. Another disadvantage is the need for a graft–graft anastomosis, which is fortunately easy with a good view taking 5–10 min.

References

[1] Bachet J, Guilmet D, Goudot B, Dreyfus GD, Delentdecker P, Brodaty D, Dubois C. Antegrade cerebral perfusion with cold blood: a 13-year experience. Ann Thorac Surg 1999;67:1874–8.
[2] Kazui T, Washiyama N, Muhammad BA, Terada H, Yamashita K, Takinami M. Total arch replacement using aortic arch branched grafts with the aid of antegrade selective cerebral perfusion. Ann Thorac Surg 2000;70(1):3–8.
[3] Kazui T, Washiyama N, Muhammad BA, Terada H, Yamashita K, Takinami M. Improved results of atherosclerotic arch aneurysm operations with a refined technique. J Thorac Cardiovasc Surg 2001;121(3):491–9.
[4] Kazui T, Yamashita K, Washiyama N, Terada H, Bashar AH, Suzuki T, Ohkura K. Usefulness of antegrade selective cerebral perfusion during aortic arch operations. Ann Thorac Surg 2002;74(5):S1806–9.
[5] Takamoto S, Okita Y, Ando M, Morota T, Handa N, Kawashima Y. Retrograde cerebral circulation for distal aortic arch surgery through a left thoracotomy. J Card Surg 1994;9(5):576–82 [discussion 582–3].
[6] Ogino H, Ueda Y, Sugita T, Matsuyama K, Matsubayashi K, Nomoto T, Yoshioka T. Aortic arch repairs through three different approaches. Eur J Cardiothorac Surg 2001;19(1):25–9.
[7] Westaby S, Katsumata T. Proximal aortic perfusion for complex arch and descending aortic disease. J Thorac Cardiovasc Surg 1998;115:162–7.
[8] Numata S, Ogino H, Sasaki H, Hanafusa Y, Hirata M, Ando M, Kitamura S. Total arch replacement using antegrade selective cerebral perfusion with right axillary artery perfusion. Eur J Cardiothorac Surg 2003;23(5):771–5.

Is Emergency Total Arch Replacement With a Modified Elephant Trunk Technique Justified for Acute Type A Aortic Dissection?

Hirotaka Watanuki, MD, Hitoshi Ogino, MD, Kenji Minatoya, MD, Hitoshi Matsuda, MD, Hiroaki Sasaki, MD, Motomi Ando, MD, and Soichiro Kitamura, MD

Department of Cardiovascular Surgery, National Cardiovascular Center, and Department of Thoracic Surgery, Fujita Health University, Osaka, Japan

Background. We assess the outcome of emergency total arch replacement with a modified elephant trunk technique for acute type A aortic dissection to clarify whether our aggressive approach is justified in certain patients.

Methods. Between 2000 and 2006, 54 patients (55.1% of all) underwent emergency total arch replacement for acute type A aortic dissection. The surgery was performed using open distal anastomosis with selective antegrade cerebral perfusion under hypothermia. Total arch replacement with individual arch-vessel reconstruction was applied in the following settings: the intimal tear in the transverse arch or the proximal descending aorta, massive arch dissection, Marfan syndrome, arch aneurysm, and atheromatous arch. At the distal anastomosis, a modified elephant trunk procedure was added for secure anastomosis and early thrombosed closure of the false channel in the descending aorta.

Results. Only 2 patients (3.7%) died of low cardiac output, in whom cardiac arrest had developed preoperatively owing to rupture of the arch or to left coronary artery malperfusion. There were 4 late deaths from non-aortic events. On the follow-up computed tomographic scanning, a high incidence of early thrombosed closure of the false channel in the dissected descending aorta was found. Only 2 patients, whose tear had not been resected in the first surgery, required reoperation of the descending aorta.

Conclusions. Total arch replacement with an elephant trunk procedure, which permits immediate survival and provides early thrombosed closure of the distal false channel, is justified in certain patients with acute type A dissection.

(Ann Thorac Surg 2007;84:1585–91)

Acute type A aortic dissection is a potentially catastrophic event and requires surgical repair on an emergency basis. Despite recent favorable outcomes by leading centers [1, 2], the surgery still has a high mortality rate of 14% to 32.5% [3–6]. In these circumstances, limited ascending aortic or hemiarch replacement is widely accepted to permit a primary goal of immediate survival by preventing secondary cardiac events. However, the residual dissection's behavior in the aortic arch or thoracoabdominal aorta after the limited repair is still unclear. In the long term, repeated surgery for the residual dissection of the arch, descending thoracic aorta, and abdominal aorta would be necessary in some instances [7, 8]. Extended total arch repair is then more advantageous for complete resection of the intimal tear and the massively dissected arch [9]. In particular, with a modified elephant trunk technique, total arch repair might be more beneficial to prevent late enlargement of the residual aortic dissection.

In this study, we evaluated the early and midterm outcome of emergency total arch replacement with a modified elephant trunk technique for acute type A aortic dissection to clarify whether our aggressive approach is justified in certain patients who would have potential for enlargement of the distal dissection.

Patients and Methods

Patients

Between 2000 and 2006, a total of 98 patients underwent emergent or urgent surgery for acute type A aortic dissection in the National Cardiovascular Center, Japan. Extended total arch replacement was performed in 54 patients (55.1%) of them (Table 1). One patient had previous history of type B dissection. Another patient developing significant distal anastomotic leak immediately after emergent hemiarch replacement was also included, although patients having iatrogenic dissection were excluded. Other 40 patients underwent hemiarch replacement and 4 patients partial arch replacement with reconstruction of the innominate artery. The institutional

Accepted for publication June 15, 2007.

Presented at the Poster Session of the Forty-third Annual Meeting of The Society of Thoracic Surgeons, San Diego, CA, Jan 29–31, 2007.

Address correspondence to Dr Ogino, Department of Cardiovascular Surgery, National Cardiovascular Center, 5-7-1 Fujishirodai, Suita, Osaka, 565-8565, Japan; e-mail: hogino@hsp.ncvc.go.jp.

Published by Elsevier Inc

Table 1. Preoperative Patient Characteristics

Characteristic	Value
Age (years)	66 (28–86)
Sex (male/female)	30/24
Marfan syndrome (n)	3
Onset to surgery (n)	
Within 6 hours	24
6–24 hours	22
1–7 days	4
1–2 weeks	4
Surgery (n)	
Emergent	51
Urgent	3
Persistent malperfusion (n)	11 (20.4%)
Brain	2
Heart (coronary)	1
Bowel (SMA)	1
Limb (arm/leg)	7 (4/3)
Cardiac tamponade (n)	16 (29.6%)
Aortic valve insufficiency, grade ≥III (n)	11 (20.4%)
Shock, blood pressure ≤80 mm Hg (n)	13 (26.3%)
Cardiac arrest on CPR	4
Rupture (n)	9 (16.7%)
Patent false channel (n)	48 (88.9%)
Range of dissection (n)	
Ascending–descending aorta	49 (90.7%)
Ascending aorta–arch	5
Location of the intimal tear (n)	
Ascending aorta	23
Arch	18
Descending aorta	13

CPR = cardiopulmonary resuscitation; SMA = superior mesenteric artery.

approval for this study was obtained, and each patient within the study gave informed consent for serving as a subject.

Surgical Technique

CARDIOPULMONARY BYPASS WITH ADDITIONAL AXILLARY ARTERY PERFUSION. With standard retrograde perfusion through the femoral artery, an additional right axillary artery perfusion was used for maintaining the true channel circulation and easy shift to selective antegrade cerebral perfusion (SCP [Fig 1]) [10]. The right axillary artery was quickly exposed and easily cannulated in the axilla, to where arterial dissection hardly extends. A 10F to 16F thin-wall cannula was inserted. The femoral artery was also cannulated with a 16F to 21F cannula. Bicaval venous drainage with left ventricular venting was used.

BRAIN PROTECTION. Patients were cooled to the range of 20°C to 28°C (Fig 1). With hypothermic circulatory arrest, SCP through the right axillary artery was quickly commenced by clamping the innominate artery. The ascending aorta was opened without aortic clamp. The site and extent of intimal tear was defined. A SCP balloon-tipped cannula was inserted into the left common carotid artery with the left subclavian artery clamped. During the SCP, the superficial temporal artery or the balloon-tip pressures were regulated in the range of 30 to 50 mm Hg by the SCP flow of approximately 10 to 12 mL · kg^{-1} · min^{-1}. Since 2003, the left subclavian artery perfusion has been included with moderate hypothermia. The SCP flow was also increased to maintain the pressure at approximately 50 mm Hg.

TOTAL ARCH REPLACEMENT WITH A MODIFIED ELEPHANT TRUNK TECHNIQUE. Ascending aortic or hemiarch replacement was the procedure principally performed for our tear-oriented surgery (Fig 1) [1, 2]. With hypothermic circulatory arrest, the ascending aorta was transected proximal to the innominate artery, excising a tear. With a tear in the minor arch curvature, the arch including a tear was beveled for hemiarch replacement. The false channel was closed with internal and external Teflon felt strips. A 22 mm to 26 mm single-branched Dacron graft was anastomosed with an open aortic technique. The antegrade distal aortic perfusion was commenced using the branch graft, and the patient was rewarmed. In contrast, extended total arch replacement with a modified elephant trunk technique [11] was attempted in the following settings: (1) tear (entry) in the arch (excluding the minor curvature); (2) tear in the descending aorta ("retrograde dissection"); (3) reentry in the arch or the proximal descending aorta; (4) Marfan syndrome; (5) arch aneurysm or dilatation; (6) atheromatous arch; (7) massive arch dissection; and (8) relatively young age less than 70 years [9, 12, 13].

In total arch replacement, the descending aorta was transected distal to the left subclavian artery. A modified elephant trunk technique was used for secure anastomosis with less anastomotic bleeding and early thrombosed

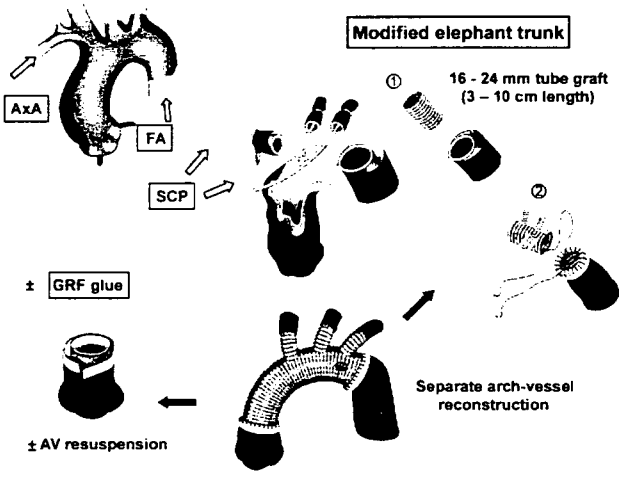

Fig 1. Total arch replacement with a modified elephant trunk technique using antegrade selective cerebral perfusion (SCP) with right axillary artery (AxA) perfusion. (AV = aortic valve; FA = femoral artery; GRF-glue = Gelatin-Resorcin-Formal glue.)

closure of the distal false channel [12, 13] . Depending on the size and condition of the true channel in the descending aorta, a prosthetic graft of 16 mm to 24 mm in diameter and 3 cm to 10 cm in length was carefully inserted into the distal true channel. The proximal end of the elephant trunk graft was attached to the completely divided descending aorta using a 4-0 polypropylene continuous suture. The anastomosis was reinforced by an external Teflon felt strip. Another quadrifurcated Dacron arch graft of 20 to 24 mm in diameter was anastomosed to this aortic stump with a 4-0 polypropylene continuous suture. The antegrade distal aortic perfusion was commenced with a branch graft of the arch graft.

By transesophageal echocardiography, good shape of the inserted elephant trunk graft without kinking was confirmed. The left subclavian artery was reconstructed using a branch graft with the reinforcement of an external felt. The patient was then rewarmed. At the proximal site, the ascending aorta was transected just around the sinotubular junction. The proximal false channel was closed with internal and external Teflon felt strips. When the commissures of aortic valve detached, they were attached using 5-0 polypropylene pledgeted mattress sutures in 25 patients. In most, the proximal false channel was fixed using Gelatin-Resorcin-Formal glue (Cardial, Sainte-Etienne, France) [3]. In a recent 5 patients, an adventitial inversion technique was used without Gelatin-Resorcin-Formal glue. The main graft was anastomosed to this end with a 4-0 polypropylene continuous suture. Finally, the other two arch vessels were reconstructed using branch grafts with 5-0 polypropylene continuous suture under SCP.

Data Collection and Statistical Analysis

Medical records were reviewed. All patients have been followed at our outpatient clinic at intervals of 3 to 12 months. The follow-up rate was 100%, and the mean duration was 2.9 ± 1.8 years. We reviewed the early and midterm outcomes and investigated risk factors for in-hospital mortality and for reoperation of the distal dissection by univariate and multivariate analyses, which were carried out using SPSS software (SPSS, Chicago, Illinois). Values are expressed as the mean ± SD or medians (range), with p values less than 0.05 considered significant. Univariate analysis was carried out using the χ^2 test or Fisher exact test. Stepwise logistic regression was used for multivariate analysis. A logistic regression model was used with p less than 0.10 as the limit for selecting variables for entry into the model. Kaplan-Meier estimates were used to calculate long-term survival and reoperation-free rates.

In the follow-up, enhanced computed tomography (CT) scanning of the entire aorta was undertaken annually to assess late enlargement of the distal dissection and the fate of the distal false channel. The diameter of the dissected aorta was measured on the short-axis view at four points of the proximal, middle, and distal descending aorta, and the abdominal aorta around the origin of the superior mesenteric artery. The conditions of the false lumen were evaluated using three grades: (1) thrombosed closure, (2) nearly closed with most of parts thrombosed, and (3) patent. The authors had full access to the data and take responsibility for its integrity. All authors have read and agree to the manuscript as written.

Results

Total arch replacement was performed in certain patients with the following settings: tear in the arch (n = 18), tear in the descending aorta (13), massive arch dissection (17), Marfan syndrome (2), arch aneurysm (1), atheromatous arch (1), distal end of dissection in the arch (2), arch rupture (1), and descending aortic rupture (1). Concomitantly, aortic valve resuspension (n = 25), composite root replacement (2), valve-sparing root surgery (3), aortic valve replacement (1), mitral valve plasty (1), coronary artery bypass grafting (5), and ascending aorta to external iliac or femoral artery bypass for limb ischemia (2) were performed. The median duration of open distal anastomosis, cardiac arrest, SCP, cardiopulmonary bypass, and surgery was 55.5 minutes (range, 34 to 130), 136.5 minutes (84 to 379), 167.5 minutes (50 to 455), 236 minutes (124 to 789), and 462.5 minutes (237 to 1,375). The stay in the intensive care unit and the hospital was 5 days (range, 1 to 52) and 31.5 days (16 to 130), respectively. The amount of transfusion was 3,780 mL (range, 0 to 20,000 mL).

The following complications occurred: bleeding in 5.6% (n = 3), cardiac in 5.6% (3), respiratory in 13.0% (7), renal in 1.9% (1), hepatic in 1.9% (1), gastrointestinal tract in 1.9% (1), limb (leg) ischemia in 3.7% (2), infection in 1.9% (1), and wound in 1.9% (1). Cerebral deficits occurred in 11.1% (6): temporary neurologic dysfunction in 5.6% (3) and permanent dysfunction in 5.6% (3). One severe permanent neurologic dysfunction was due to preoperative cardiac arrest in the anesthetic induction owing to rupture, and cardiac massage was required until the establishment of cardiopulmonary bypass. The other 2 permanent dysfunctions were presumably due to preoperative serious cerebral malperfusion caused by extended dissection of the innominate artery to the right common carotid artery. The surgery needed to be rushed for cardiac tamponade, although both of the patients were unconscious. These 2 patients rehabilitated eventually.

There were two 30-day deaths (3.7%) due to low cardiac output. Both of these 2 female patients with preoperative deep shock had fallen into cardiac arrest during the anesthetic induction owing to ascending aorta to aortic arch rupture in 1 patient or to coronary malperfusion in 1 patient. For the first patient, hemiarch replacement was initially attempted because all of the three intimal tears were located in the ascending aorta. However, rupture of the transverse arch close to the arch vessels was found after the proximal anastomosis so that total arch replacement was performed after recooling the patient. This patient had severe edema of the whole body and abdominal distension associated with severe acidosis; she did

Ann Thorac Surg
2007;84:1585–91

Table 2. Univariate Analysis of Risk Factors for In-Hospital Mortality

Factor	*p* Value
Super acute (≤6 hours from onset)	0.872
Female	0.193
Age ≥70 years	0.508
Marfan syndrome	0.727
Cardiac tamponade	0.509
Shock (blood pressure ≤80 mm Hg)	0.055
Cardiac arrest before surgery	0.004[a]
Aortic valve insufficiency (≥III)	0.466
Rupture	0.308
Tear in arch/descending aorta	0.915
Malperfusion	0.370
Coronary malperfusion	0.037[a]
Patent false channel	0.610
Concomitant surgery	0.369
Open distal anastomosis ≥60 minutes	0.177
Cardiac arrest ≥180 minutes	0.039[a]
Cardiopulmonary bypass ≥5 hours	0.073
Surgery ≥10 hours	0.055
Blood transfusion ≥5,000 mL	0.161

[a] $p < 0.05$.

not recover despite cardiopulmonary support using femorofemoral circuit. In the second patient, having deep shock and severe pulmonary congestion due to left coronary malperfusion preoperatively, severe hypokinesis of the anteroseptal wall with left ventricular dilatation and mitral regurgitation of grade IV due to left coronary malperfusion were revealed on transthoracic echocardiography. Total arch repair was carried out because of the primary tear located in the transverse arch just close to the left common carotid artery. After that, at the proximal site, routine supracoronary anastomosis was done with Gelatin-Resorcin-Formal glue. However, after the anastomosis, rupture of the right coronary artery due to extension of the dissection was noticed. Full root repair was carried out using a porcine stentless valved graft. However, cardiac function did not recover despite intra-

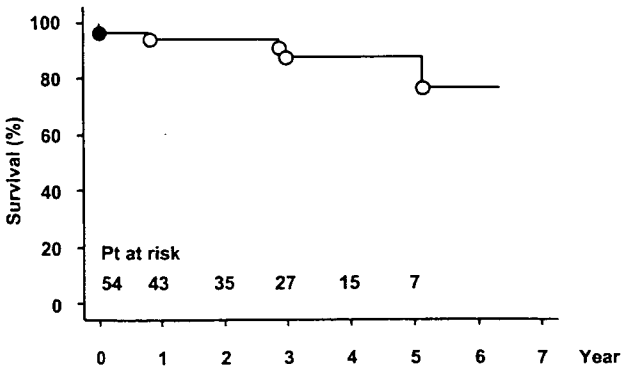

Fig 2. Midterm survival, Kaplan-Meier method. (Pt = patients.)

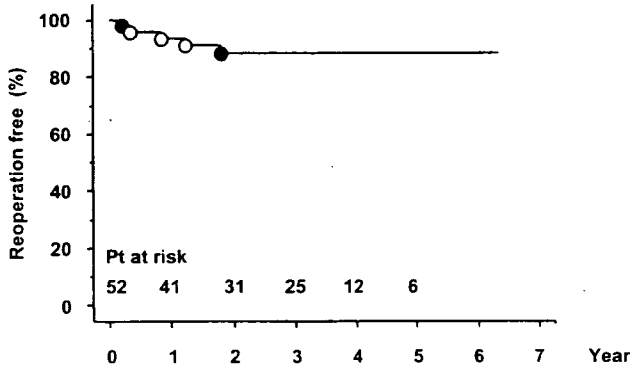

Fig 3. Freedom from reoperation, Kaplan-Meier method. (Open circles = replacement of root [2] or ascending aorta [1]; solid circles = replacement of descending aorta [2]; Pt = patients.)

aortic balloon pumping and percutaneous cardiopulmonary support using a femorofemoral circuit.

On the univariate analysis, significant risk factors for 30-day mortality were cardiac arrest before surgery, coronary malperfusion, and the duration of cardioplegic cardiac arrest more than 180 minutes (Table 2). In the following multivariate analysis, no independent predictors for mortality were found.

During the mean follow-up period of 2.9 ± 1.8 years, 4 late deaths (7.8%) occurred from nonaortic events such as pneumonia (n = 2), cancer (1), and suicide (1; Fig 2). The actuarial survival including hospital deaths was 87.8% ± 1.2% at 3 years. Five patients (9.6%) required reoperation: root replacement for recurrent aortic regurgitation (n = 2), ascending aortic replacement for proximal anastomotic stricture due to the internal felt strip (1), and descending replacement (2; Fig 3). Regarding the reoperation of the distal dissection with the incidence of 3.8%, 1 of the 2 patients had suffered from type B aortic dissection before acute type A dissection. In the total arch replacement for new type A dissection, the previous tear of old dissection in the descending aorta was not resected, resulting in the enlargement of the descending aorta. Another patient had the tear in the descending aorta, which was not noticed through a median approach. The tear was not resected in the total arch repair, resulting in the descending aortic dilatation. The overall reoperation-free rate was 88.4% ± 11.7% at 3 years. On univariate analysis, no resection of the tear in the de-

Table 3. Univariate Analysis of Risk Factors for Reoperation of the Descending Aorta

Factor	*p* Value
Patent false channel before surgery	0.610
Marfan syndrome	0.727
Tear in the descending aorta	0.427
No tear resection	0.004[a]
Patent false channel in the proximal descending aorta	0.144

[a] $p < 0.05$.

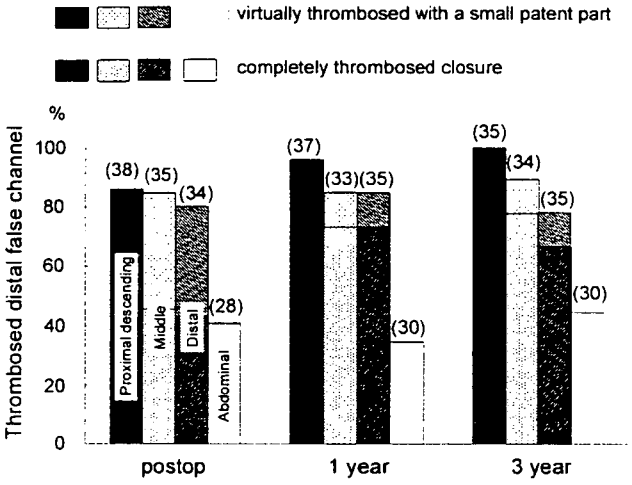

Fig 4. Behavior of distal false channels after total arch replacement with a modified elephant trunk technique on the follow-up computed tomography scans. Numbers in parentheses indicate median diameter of the distal dissected aorta including true and false channels. (Postop = postoperative, before discharge.)

scending aorta was a risk factor for distal aortic reoperation (Table 3).

The follow-up CT scans showed early thrombosed closure of the distal false channel (Fig 4). Particularly, in the proximal, middle, and distal descending aorta, the complete thrombosis was demonstrated at the incidence of 43.2%, 45.5%, and 43.2% immediately after the surgery (n = 49); 84.6%, 73.1%, and 77.8% in 1 year (n = 34); and 100%, 77.8%, and 66.7% in 3 years (n = 21). Including the condition of nearly closed with most of parts thrombosed, the rate of thrombosed closure of the distal false channel was 88.6%%, 84.1%, and 79.5% immediately after the surgery; 92.3%, 84.6%, and 84.6% in 1 year; and 100%, 88.9%, and 77.8% in 3 years.

Comment

The outcome of total arch replacement with a modified elephant trunk under SCP with axillary artery perfusion was satisfactory, with a low in-hospital mortality rate. The primary goal of emergency surgery for acute type A aortic dissection is to save patients' lives. Limited ascending aortic or hemiarch replacement is then widely recommended [1–6]. With recent advances of diagnosis and surgery, the outcome has improved to less than 10% mortality in the leading centers [1, 2]. In our institution, the overall mortality in emergency surgery for acute type A aortic dissection, including ascending or hemiarch repair, was 2.9% during the same period. The in-hospital mortality rate in extended total arch replacement was 3.7%, which did not increase dramatically. This satisfactory outcome is, we believe, based on our surgical background consisting of a large number of arch surgeries [10, 14, 15]. During the same period, a total of 458 patients underwent total arch replacement for a variety of aortic pathologies including chronic dissecting and nondissecting aneurysms. The in-hospital mortality rate for elective total arch replacement for nondissecting aneurysm in 305 patients was 2.3% [15].

For arch surgery, we have established an integrated circulatory support system consisting of axillary artery perfusion for cardiopulmonary bypass coupled with femoral artery or ascending aortic perfusion and of SCP [10, 14, 15]. In particular, we have advocated routine use of axillary artery perfusion [10]. The exposure of the distal part of axillary artery in the axilla is quicker and easier than that in the subclavicular region. Arterial dissection rarely extends to this portion of the axillary artery. Secure perfusion of the true channel can be commenced quickly, improving cardiac and cerebral safety. Furthermore, easy shift to the SCP is feasible by clamping the innominate artery without cannulation. Our increasing experiences with arch replacement using SCP with the axillary artery perfusion has led to our growing confidence in the safe application of this prompt approach of total arch replacement even on an emergency basis [10, 13–15].

Previous reports identified various risk factors for mortality such as early year operation, increasing age, history of aortic valve replacement, high New York Heart Association class, diabetes mellitus, shock, cardiac tamponade, rupture, coronary malperfusion, visceral malperfusion, limb malperfusion, root replacement, arch replacement, coronary artery bypass graft surgery, or longer circulatory arrest [4–6]. In the presented series, cardiac arrest before surgery as well as coronary malperfusion was a risk factor for in-hospital mortality in the univariate analysis. It was extremely difficult to rescue these 2 critical patients having serious coronary malperfusion or aortic arch rupture. Given a larger number of such critical patients, the outcome might have been much worse with a higher mortality.

Complete resection of the primary tear is a key to good early and long-term outcomes. In previous reports, no differences were recognized in mortality or reoperation rate whether the tear was resected or not [16, 17]. However, subsequent reports noted that the reoperation rate was significantly higher without tear resection [3, 18–20]. Since then, "tear-oriented surgery" has been widely recommended [1–6]. In previous studies, anastomotic leakage, no tear resection, younger age, Marfan syndrome, and severe aortic regurgitation were significant determinants for reoperation [3, 18–22]. Given a tear in the arch excluding the minor curvature site or in the proximal descending aorta, total arch replacement is then reasonable [3, 13, 18, 19, 21, 22]. Furthermore, in cases with massive arch dissection, complete arch replacement would be more beneficial to avoid bleeding, anastomotic leak, progression of aneurysmal dilatation, rupture, reoperation, and cerebral malperfusion [3, 18, 19]. Recently, the Mount Sinai group [22] described that repeated surgical intervention was most frequently required in the aortic arch and abdominal aorta in a large series. We believe our aggressive total arch replacement for complete resection of massive arch dissection as well as the primary tear can reduce the incidence of distal reoperation, in particular, for arch dilatation.

Coupled with the total arch repair, a modified elephant trunk technique was used for secure anastomosis and for early thrombosed closure of the distal false channel [11, 12]. Without the internal reinforcement by elephant trunk graft, the distal anastomosis would be more troublesome with bleeding because of a fragile dissected descending aorta. Literally, the patent false channel was recognized in the incidence of approximately 50% to 80% after the conventional ascending aortic replacement. In our series, having total arch repair with a modified elephant trunk, early thrombosed closure or obliteration of the false channel in the descending aorta was recognized frequently on the follow up CT scans. From this point of view, we believe this unique technique plays an important role or is essential for total arch replacement for acute type A dissection [12]. It does, however, have some shortcomings. The true channel in the descending aorta is generally too small to accept a large-size graft, making necessary the use of another smaller-size graft. With such a size mismatch, the inserted elephant trunk graft might be kinked or wrinkled, resulting in stenosis or hemolysis. Its adequate length is also unknown. The longer the graft is, the greater the impact of elephant trunk on closure or obliteration of the distal false channel is. However, with a too-long elephant trunk, the potential risk of spinal cord injury or new tear formation would increase [23]. Regardless, we propose as another advantage, with the elephant trunk, that the reoperation of the descending aorta would be much easier [11, 12]. The elephant trunk procedure should be coupled with total arch replacement.

The aim of the elephant trunk procedure was to reduce the reoperation rate by preventing enlargement of the distal dissected aorta. However, 2 patients, whose tear had not been resected in the first surgery, required descending aortic replacement in the late stage. In 1 patient having the tear in the descending aorta that was not noticed intraoperatively, the elephant trunk was 5 cm in length. It was subsequently too short to cover the tear. If the tear had been identified, we could have closed the tear using a longer elephant trunk. Kato and colleagues [24] and Ishihara and associates [25] reported greater impact of stent graft as an elephant trunk on closing the false channel, instead of standard prosthetic graft. However, in the use of stent graft for acute aortic dissection, a potential risk of new intimal tear formation exists [26]. More flexible stent graft might be preferable for such fragile aortic wall of acute dissection. For reoperation of the descending aorta, patent false channel, anastomotic leakage, no tear resection, younger age, and Marfan syndrome were reportedly risk factors [3, 18, 19]. In this series, reoperation of the descending aorta was required only in the 2 cases without resection of the tear in the descending aorta. For such patients having a potential risk of distal dilatation, meticulous follow up using CT scans is mandatory.

Postoperative cerebral morbidity remains one of the critical complications, particularly in total arch repair requiring longer SCP. Generally, the incidence is higher compared with ascending or hemiarch repair. In total, 3 patients had strokes due to brain damage during cardiac resuscitation or to preoperative cerebral malperfusion. Although 2 patients having cerebral malperfusion were unconscious before surgery, the surgery was indicated because brain CT scans did not reveal any infarction.

This retrospective study has some limitations. The number of patients might be too small to reach definitive conclusions. For that, a larger number of patients is necessary. There was no appropriate control group having ascending or hemiarch replacement, because the limited repairs were performed in the patient group having different conditions including the site of the primary tear. For definitive conclusions, a randomized controlled study is required between the extended and limited repairs in patients having homogenous aortic lesions.

In conclusion, total arch replacement with a modified elephant trunk procedure under SCP with right axillary artery perfusion, which permits immediate survival and can reduce the distal aortic reoperation rate, would be justified in certain patients with acute type A aortic dissection.

References

1. Westaby S, Saito S, Katsumata T. Acute type A dissection: conservative methods provide consistently low mortality. Ann Thorac Surg 2002;73:707–13.
2. Bavaria JE, Brinster DR, Gorman RC, et al. Advances in the treatment of acute type A dissection: an integrated approach. Ann Thorac Surg 2002;74(Suppl):1848–52.
3. Bachet J, Goudot B, Guilmet D, et al. Surgery for acute type A aortic dissection: the Hospital Foch experience (1977–1998). Ann Thorac Surg 1999;67:2006–9.
4. Ehrlich MP, Ergin MA, Griepp RB, et al. Results of immediate surgical treatment of all acute type A dissections. Circulation 2000;102(Suppl 3):248–52.
5. Mehta RH, Nienaber CA, Eagle KA, et al, and the International Registry of Acute Aortic Dissection (IRAD) Investigators. Predicting death in patients with acute type A aortic dissection. Circulation 2002;105:200–6.
6. Trimarchi S, Nienaber CA, Rampoldi V, et al, and the International Registry of Acute Aortic Dissection Investigators. Contemporary results of surgery in acute type A aortic dissection: the International Registry of Acute Aortic Dissection experience. J Thorac Cardiovasc Surg 2005;129:112–22.
7. Bachet J, Termingnon JL, Goudot B, et al. Late reoperations in patients with aortic dissection. J Card Surg 1994;9:740–6.
8. Kirsch M, Soustelle C, Houël R, et al. Risk factor analysis for proximal and distal reoperations after surgery for acute type A aortic dissection. J Thorac Cardiovasc Surg 2002;123:318–25.
9. Kazui T, Yamashita K, Washiyama N, et al. Impact of an aggressive surgical approach on surgical outcome in type A aortic dissection. Ann Thorac Surg 2002;74(Suppl):1844–7.
10. Numata S, Ogino H, Ando M, et al. Total arch replacement using antegrade selective cerebral perfusion with right axillary artery perfusion. Eur J Cardiothorac Surg 2003;23:771–5.
11. Borst HG, Frank G, Schaps D. Treatment of extensive aortic aneurysms by a new multiple-stage approach. J Thorac Cardiovasc Surg 1988;95:11–3.
12. Ando M, Takamoto S, Okita Y, et al. Elephant trunk procedure for surgical treatment of aortic dissection. Ann Thorac Surg 1998;66:82–7.
13. Hanafusa Y, Ogino H, Sasaki H, et al. Total arch replacement with elephant trunk procedure for retrograde dissection. Ann Thorac Surg 2002;74(Suppl):1836–9.

14. Minatoya K, Ogino H, Matsuda H, et al. Surgical management of distal arch aneurysm: another approach with improved results. Ann Thorac Surg 2006;81:1353–7.
15. Sasaki H, Ogino H, Matsuda H, et al. Integrated total arch replacement using selective cerebral perfusion: a six-year experience. Ann Thorac Surg 2007;83:S805–10.
16. Miller DC, Mitchell RS, Oyer PE, et al. Independent determinants of operative mortality for patients with aortic dissections. Circulation 1984;70(Suppl):I153–64.
17. Haverich A, Miller DC, Scott WC, et al. Acute and chronic aortic dissections—determinants of long-term outcome for operative survivors. Circulation 1985;72(Suppl):II22–34.
18. Kazui T, Washiyama N, Bashar AH, et al. Surgical outcome of acute type A aortic dissection: analysis of risk factors. Ann Thorac Surg 2002;74:75–81.
19. Moon MR, Sundt TM III, Pasque MK, et al. Does the extent of proximal or distal resection influence outcome for type A dissections. Ann Thorac Surg 2001;71:1244–50.
20. Heinemann M, Laas J, Borst HG, et al. Surgery extended into the aortic arch in acute type A dissection. Indications, techniques, and results. Circulation 1991;84(Suppl 3):25–30.
21. Crawford ES, Kirklin JW, Naftel DC, et al. Surgery for acute dissection of ascending aorta. Should the arch be included? J Thorac Cardiovasc Surg 1992;104:46–59.
22. Halstead JC, Meier M, Griepp RB, et al. The fate of the distal aorta after repair of acute type A aortic dissection. J Thorac Cardiovasc Surg 2007;133:127–35.
23. Flores J, Kunihara T, Shiiya N, et al. Extensive deployment of the stented elephant trunk is associated with an increased risk of spinal cord injury. J Thorac Cardiovasc Surg 2006;131:336–42.
24. Kato M, Kuratani T, Kaneko M, et al. The results of total arch graft implantation with open stent-graft placement for type A aortic dissection. J Thorac Cardiovasc Surg 2002;124:531–40.
25. Ishihara H, Uchida N, Yamasaki C, et al. Extensive primary repair of the thoracic aorta in Stanford type A acute aortic dissection by means of a synthetic vascular graft with a self-expandable stent. J Thorac Cardiovasc Surg 2002;123:1035–40.
26. Shimono T, Kato N, Yasuda F, et al. Transluminal stent-graft placements for the treatments of acute onset and chronic aortic dissections. Circulation 2002;106(Suppl 1):241–7.

Journal of Thrombosis and Haemostasis, 3: 2315–2323

ORIGINAL ARTICLE

Impaired platelet function in a patient with $P2Y_{12}$ deficiency caused by a mutation in the translation initiation codon

M. SHIRAGA,* S. MIYATA,† H. KATO,* H. KASHIWAGI,* S. HONDA,* Y. KURATA,‡ Y. TOMIYAMA* and Y. KANAKURA*

**Department of Hematology and Oncology, Graduate School of Medicine C9, Osaka University, Osaka, Japan; †Division of Blood Transfusion Medicine, National Cardiovascular Center, Osaka, Japan; and ‡Department of Blood Transfusion, Osaka University Hospital, Osaka, Japan*

To cite this article: Shiraga M, Miyata S, Kato H, Kashiwagi H, Honda S, Kurata Y, Tomiyama Y, Kanakura Y. Impaired platelet function in a patient with $P2Y_{12}$ deficiency caused by a mutation in the translation initiation codon. *J Thromb Haemost* 2005; 3: 2315–23.

Summary. In this study, we have identified a patient (OSP-1) with a congenital $P2Y_{12}$ deficiency showing a mild bleeding tendency from her childhood and examined the role of $P2Y_{12}$ in platelet function. At low concentrations of agonists OSP-1 platelets showed an impaired aggregation to several kinds of stimuli, whereas at high concentrations they showed a specifically impaired platelet aggregation to adenosine diphosphate (ADP). ADP normally induced platelet shape change and failed to inhibit PGE_1-stimulated cAMP accumulation in OSP-1 platelets. Molecular genetic analysis revealed that OSP-1 was a homozygous for a mutation in the translation initiation codon (ATG to AGG) in the *P2Y*$_{12}$ gene. Heterologous cell expression of wild-type or mutant $P2Y_{12}$ confirmed that the mutation was responsible for the deficiency in $P2Y_{12}$. OSP-1 platelets showed a markedly impaired platelet spreading onto immobilized fibrinogen. Real-time observations of thrombogenesis under a high shear rate (2000 s^{-1}) revealed that thrombi over collagen were small and loosely packed and most of the aggregates were unable to resist against high shear stress in OSP-1. Our data suggest that secretion of endogenous ADP and subsequent $P2Y_{12}$-mediated signaling are critical for platelet aggregation, platelet spreading, and as a consequence, for stabilization of thrombus.

Keywords: $\alpha_{IIb}\beta_3$, initiation codon, mutation, $P2Y_{12}$ deficiency, platelets, thrombogenesis.

Introduction

Platelets play a crucial role not only in a hemostatic plug formation, but also in a pathologic thrombus formation, particularly within atherosclerotic arteries subjected to high shear stress [1,2]. As an initial step in thrombogenesis, platelets adhere to exposed subendothelial matrices such as von Willebrand factor (VWF) and collagen, then become activated and aggregate to each other. These processes are primarily mediated by platelet surface glycoproteins such as GPIb-IX-V, $\alpha_2\beta_1$, GPVI, and $\alpha_{IIb}\beta_3$ (GPIIb-IIIa) [3,4]. In addition, several mediators such as adenosine diphosphate (ADP), thromboxane A_2, and thrombin cause further platelet activation and recruitment of circulating platelets to the injury sites through activation of $\alpha_{IIb}\beta_3$ and subsequent binding of VWF and fibrinogen.

Recent studies have demonstrated a critical role for ADP in arterial thrombogenesis [5–7]. ADP is actively secreted from platelet dense granules on platelet activation and is passively released from damaged erythrocytes and endothelial cells. Platelets possess at least two major G protein-coupled ADP receptors that are largely responsible for platelet responses to ADP: $P2Y_1$ and $P2Y_{12}$ [6]. $P2Y_1$ is the G_q-coupled receptor responsible for mediating platelet shape change and reversible platelet aggregation through intracellular calcium mobilization [8,9], whereas $P2Y_{12}$ is the G_i-coupled receptor responsible for mediating inhibition of adenylyl cyclase and sustained platelet aggregation [10–12]. $P2Y_{12}$ is the therapeutic target of efficacious antithrombotic agents, such as ticlopidine, clopidogrel, and AR-C compounds [5,6], and its congenital deficiency results in a bleeding disorder [13,14]. The analyses of patients with $P2Y_{12}$ deficiency as well as $P2Y_{12}$-null mice would provide more precise information about the role of $P2Y_{12}$ in platelet function than those using $P2Y_{12}$ inhibitors. To date, four different families with a defect in the expression or the function of $P2Y_{12}$ have been characterized [10,13–16]. In this study, we have described a patient with the congenital $P2Y_{12}$ deficiency due to a homozygous mutation in the translation initiation codon and analyzed the role of $P2Y_{12}$ in platelet aggregation, platelet spreading onto immobilized fibrinogen, and thrombogenesis on a type I collagen-coated surface under a high shear rate. Our present data have demonstrated a crucial role of $P2Y_{12}$ in various platelet functions.

Correspondence: Yoshiaki Tomiyama, Department of Hematology and Oncology, Graduate School of Medicine C9, Osaka University, 2-2 Yamadaoka, Suita Osaka 565-0871, Japan.
Tel.: +81 6 6879 3821; fax: +81 6 6879 3879; e-mail: yoshi@hp-blood.med.osaka-u.ac.jp

Received 2 November 2004, accepted 7 June 2005

Materials and methods

Patient history

The proband (OSP-1) is a 67-year-old Japanese female with a lifelong history of easy bruising. She (OSP-1) was born from non-consanguineous parents who had no hemorrhagic diathesis. Although she showed massive bleeding during delivery of her son, she had no history of transfusions. Patient OSP-1 showed normal platelet count, normal coagulation tests (prothrombin time and activated partial thromboplastin time) and slightly elevated plasma fibrinogen (398 mg dL^{-1}). Ivy bleeding time of the patient was consistently prolonged (> 15 min). Clot retraction by MacFarlane's method was normal (50%; normal values 40%–70%). Her son never suffered from a bleeding tendency. Informed consent for analyzing their platelet function and molecular genetic abnormalities was obtained from OSP-1, her husband and their son.

Preparation of platelet-rich plasma and washed platelet suspension

Platelet-rich plasma (PRP) for aggregation studies was prepared by a centrifugation of whole blood anticoagulated with citrate at 250 *g* for 10 min and then the platelet count was adjusted at 300×10^6 mL^{-1} by platelet-poor plasma. Washed platelets were prepared as previously described [17]. In brief, 6 volumes of freshly drawn venous blood from the patient, her husband, son or healthy volunteers were mixed with 1 volume of acid–citrate–dextrose (ACD; National Institutes of Health Formula A, NIH, Bethesda, MD, USA) and centrifuged at 250 *g* for 10 min to obtain PRP. After incubation with 20 ng mL^{-1} prostaglandin E1 (PGE_1; Sigma-Aldrich, St Louis, MO, USA) for 15 min, the PRP was centrifuged at 750 *g* for 10 min, washed three times with 0.05 mol L^{-1} isotonic citrate buffer containing 20 ng mL^{-1} PGE_1 and resuspended in an appropriate buffer.

Platelet aggregometry

Platelet aggregation using PRP was monitored by a model PAM-6C platelet aggregometer (Mebanix, Tokyo, Japan) at 37 °C with a stirring rate of 1000 r.p.m. as previously described [18]. Protease-activated receptor 1-activating peptide (PAR1 TRAP, SFLLRNPNDKYEPF) and adenosine 3′,5′-diphosphate (A3P5P) were purchased from Sigma-Aldrich Corp. $P2Y_{12}$ antagonist, AR-C6993MX (2-propylthio-D-fluoromethylene adenosine 5-triphosphate) was a kind gift from AstraZeneca (Loughborough, UK).

Flow cytometry and measurement of intracellular cAMP

Flow cytometric analysis using various monoclonal antibodies (mAbs) specific for platelet membrane glycoproteins was performed as previously described [19].

For measuring intracellular cAMP levels, samples of 200 μL of washed platelets (60×10^6) in Walsh buffer (137 mM of NaCl, 2.7 mM of KCl, 1.0 mM of $MgCl_2$, 3.3 mM of NaH_2PO_4, 3.8 mM of HEPES, 0.1% of glucose, 0.1% of BSA, pH 7.4) were incubated with 1 μmol L^{-1} PGE_1 for 15 min, and then platelets were stimulated with ADP or epinephrine. After incubation for 15 min, total cellular cAMP levels were measured using the Biotrak cAMP enzyme immunoassay system from Amersham Pharmacia Biotech (Piscataway, NJ, USA).

Platelet adhesion assay

Adhesion study was performed as previously described [20]. In brief, non-treated polystyrene 10 cm dishes were coated with 100 μg mL^{-1} human fibrinogen in 5 mL of phosphate-buffered saline (PBS) at 4 °C overnight. After washing with PBS, dishes were blocked with PBS containing 1% of bovine serum albumin (BSA) for 90 min at 37 °C. Aliquots (1 mL) of washed platelets (25×10^6 mL^{-1}) were added to the fibrinogen-coated dishes and incubated at 37 °C. After incubation for 40 min, adherent platelets were fixed with 3.7% formaldehyde, permeabilized with 0.1% Triton X-100 and stained with TRITC-conjugated phalloidin. Platelet morphology and degrees of spreading were determined by fluorescence microscopy (Olympus, Tokyo, Japan).

Platelet thrombus formation under flow conditions

The real-time observation of mural thrombogenesis on a type I collagen-coated surface under a high shear rate (2000 s^{-1}) was performed as previously described [21]. In brief, type I collagen-coated glass coverslips were placed in a parallel plate flow chamber (rectangular type; flow path of 1.9-mm width, 31-mm length, and 0.1-mm height). The chamber was assembled and mounted on a microscope (BX60; Olympus, Tokyo, Japan) equipped with epifluorescent illumination (BX-FLA; Olympus) and a charge-coupled device (CCD) camera system (U-VPT-N; Olympus). Whole blood containing mepacrine-labeled platelets obtained from OSP-1 or control subjects was aspirated through the chamber by a syringe pump (Model CFV-3200, Nihon Kohden, Tokyo, Japan) at a constant flow rate of 0.285 mL min^{-1}, producing a wall shear rate of 2000 s^{-1} at 37 °C.

Amplification and analysis of platelet RNA

Total cellular RNA of platelets was isolated from 20 mL of whole blood, and $P2Y_1$ or $P2Y_{12}$ mRNA was specifically amplified by reverse transcription-polymerase chain reaction (RT-PCR), as previously described [22]. The following primers were constructed based on the published sequence of $P2Y_{12}$ cDNA and used for the first round PCR for $P2Y_{12}$ cDNA: Y12F1, 5′-GGCTGCAATAACTACTACTTACTGG-3′ [sense, nucleotide(nt) −74 to −50]; Y12R4, 5′-CAGGACAGTGTAGAGCAGTGG-3′ (antisense, nt 85 to 105) [10].

Allele-specific restriction enzyme analysis (ASRA)

Genomic DNA was isolated from mononuclear cells using SepaGene kit (Sanko Junyaku Co Ltd, Tokyo, Japan). Amplification of the region around the initiation codon of the $P2Y_{12}$ gene was performed by using primers *Bsr*DI-GF, 5′-CTTTTGTTCTCTAGGTAACCAACAAGCAA-3′ (sense, the mismatched base is underlined), and Y12R4 (antisense described above) using 250 ng of DNA as a template. These primers can be found in GenBank accession no. AC024886.20 and the sense primer corresponds to 127558–127585. PCR products were then digested with restriction enzyme *Bsr*DI. The resulting fragments were electrophoresed in a 6% polyacrylamide gel.

Construction of $P2Y_{12}$ expression vectors and cell transfection

The full-length cDNA of wild-type (WT) and mutant $P2Y_{12}$ was amplified by RT-PCR using primers Y12-*Hin*dIII-F, 5′-GAATTCAAGCTTCAAGAAATGCAAGCCGTCGACA-ACCTC-3′ (sense, nt −6 -21 for WT, *Eco*RI and *Hin*dIII sites introduced at the 5′ end were underlined) or Y12-*Hin*dIII-F2, 5′-GAATTCAAGCTTCAAGAAAGGCAAGCCGTCGAC-AACCTC-3′ (sense, nt −6 −21 for mutant), and Y12H-Not-R, 5′-TCTAGAGCGGCCGCTCAATGGTGATGGTGATGA-TGCATTGGAGTCTCTTCATT-3′ (antisense, nt 1012–1029, His × 6 were introduced before stop codon, *Not*I and *Xba*I sites introduced at the 5′ end were underlined). The amplified fragments were digested with *Hin*dIII and *Not*I, and the resulting 1059-bp fragments (nt −9 −1050) were extracted using QIAquick gel extraction kit (Qiagen, GmbH, Germany). These fragments were inserted into the pcDNA3 (Invitrogen, San Diego, CA, USA) digested with *Hin*dIII and *Not*I. The fragments inserted were characterized by sequence analysis to verify the absence of any other substitutions and the proper insertion of the PCR cartridge into the vector.

A total of 10 μg of WT or mutant $P2Y_{12}$ construct was transfected into human embryonic kidney 293 cells (HEK293 cells, 10^6 cells) using the calcium phosphate method as previously described [22]. Transfectants were lyzed by 1% Triton X-100 PBS containing protease inhibitors 2 days after transfection, and proteins were separated by 7.5% SDS-PAGE. After transferred onto a PVDF membrane, expressed proteins were detected by rabbit anti-His tag antibody.

Results

Platelet aggregation studies

We first examined the expression of platelet membrane glycoproteins in OSP-1 by flow cytometry. The patient's platelets (OSP-1 platelets) normally express GPIb-IX, $\alpha_{IIb}\beta_3$ (GPIIb-IIIa), $\alpha_2\beta_1$, and CD36 (data not shown). Fig. 1 shows platelet aggregation of PRP in response to various agonists. The aggregation of OSP-1 platelets induced by 20 μM of ADP was markedly impaired with only a small and transient

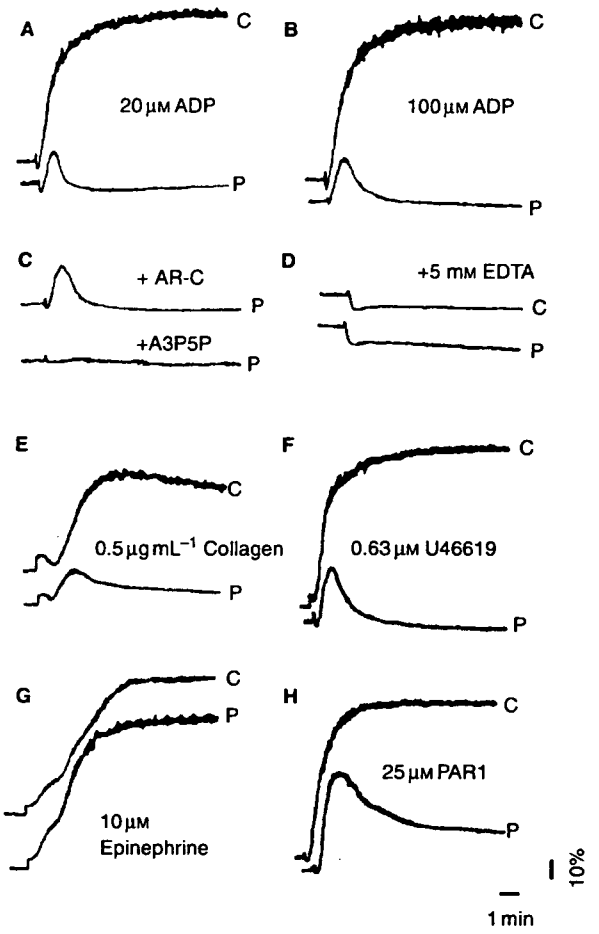

Fig. 1. Platelet aggregation induced by various agonists. Platelet aggregation was induced by various agonists in citrated PRP from patient OSP-1 (labeled 'P') or a control subject (labeled 'C'). Agonists used are (A) 20 μM of ADP, (B) 100 μM of ADP, (C) 20 μM of ADP in the presence of 1 μM of AR-C69931MX ('AR-C'), a specific $P2Y_{12}$-antagonist, or 1 mM of A3P5P ('A3P5P'), a specific $P2Y_1$-antagonist, (D) 20 μM of ADP in the presence of 5 mM of EDTA, (E) 0.5 μg mL^{-1} of collagen, (F) 0.63 μM of U46619, (G) 10 μM of epinephrine, and (H) 25 μM of PAR1-TRAP.

aggregation (Fig. 1A), and the aggregation was still impaired even at 100 μM of ADP (Fig. 1B). As compared with control platelets, the aggregation of OSP-1 platelets was also impaired with a transient aggregation in response to low concentrations of collagen (0.5 μg mL^{-1}, Fig. 1E), U46619 (0.63 μM, Fig. 1F), or PAR1 TRAP (25 μM, Fig. 1H). In response to 1.3 mg mL^{-1} ristocetin (not shown) or 10 μM of epinephrine (Fig. 1G), OSP-1 platelets aggregated normally. When OSP-1 platelets were stimulated with 20 μM of ADP in the presence of 5 mM of EDTA, the light transmission decreased equivalent to control platelets suggesting that OSP-1 platelets changed shape normally (Fig. 1D). We then examined effects of ADP receptor antagonists on the aggregation of OSP-1 platelets induced by 20 μM of ADP. A total of 1 mM of A3P5P, a specific $P2Y_1$ antagonist, abolished the residual response of OSP-1 platelets to ADP, whereas 1 μM of AR-C69931MX, a specific $P2Y_{12}$

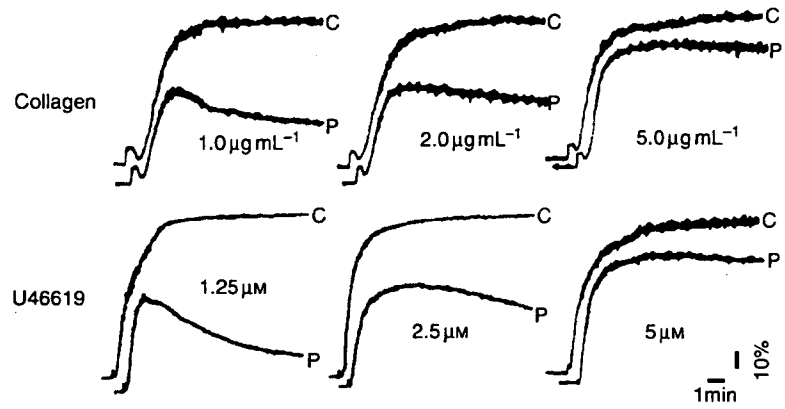

Fig. 2. Platelet aggragation induced by collagen or U46619 at various concentrations. Platelet aggregation in citrated PRP from patient OSP-1 (labeled 'P') or a control subject (labeled 'C') was induced by various concentrations of collagen or U46619. At high concentrations of collagen or U46619, OSP-1 platelets aggregate almost normally.

antagonist, did not induce an additional inhibition on the platelet aggregation (Fig. 1C). These data suggest that the impaired response of the patient's platelets may be due to an abnormality in signaling evoked by ADP and that $P2Y_{12}$-mediated signaling rather than $P2Y_1$-mediated signaling may be completely defective in patient OSP-1.

We also examined the aggregation of OSP-1 platelets induced by higher concentrations of agonists. As shown in Fig. 2, the aggregation response of OSP-1 platelets improved as the concentrations of agonists increased, and they aggregated almost normally in response to high concentrations of collagen (5 μg mL^{-1}), U46619 (5 μM), or PAR1 TRAP (100 μM) (not shown). In addition, we confirmed that 1 μM of AR-C69931MX conferred essentially the same defect on the aggregation of control platelets in response to U46619 as that of OSP-1 platelets and did not further inhibit OSP-1 platelet aggregation induced by 5 μg mL^{-1} of collagen, 5 μM of U46619, or 100 μM of PAR1 TRAP (data not shown). These data indicated that at high concentrations of agonists OSP-1 platelets showed the specifically impaired aggregation to ADP.

Effect of ADP on PGE_1-stimulated cAMP accumulation in platelets

To determine whether $P2Y_{12}$-mediated signaling is specifically impaired, we examined an inhibitory effect of ADP on 1 μM of PGE_1-stimulated cAMP accumulation in platelets from the patient, her husband, their son, and healthy unrelated controls. ADP inhibited intracellular cAMP levels in platelets from the patient's husband, son and healthy unrelated controls (not shown) by approximately 80%, whereas the inhibition was only 15% in the patient's platelets (Fig. 3). In contrast to ADP, epinephrine normally inhibited cAMP accumulation in platelets from the patient as well as her husband and son. These results strongly suggest that the defect could be due to an abnormality in G_i coupling ADP receptor, $P2Y_{12}$.

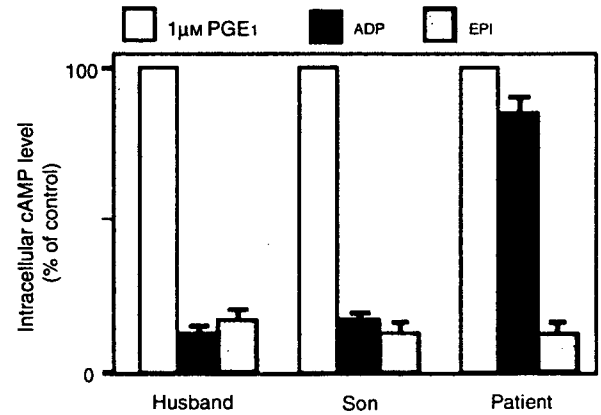

Fig. 3. Effect of ADP or epinephrine on the inhibition of PGE_1-induced cAMP accumulation in platelets. Washed platelets from patient OSP-1, husband or son were incubated with 1 μM of PGE_1 for 15 min and stimulated with 20 μM of ADP or 10 μM of epinephrine. Intracellular cAMP levels were expressed as a percent of cAMP levels in the absence of agonists. Results in OSP-1 are the mean of two experiments.

Nucleotide sequence analysis of cDNA and genomic DNA of $P2Y_{12}$

To reveal a molecular genetic defect in OSP-1, we analyzed the entire coding regions of both $P2Y_1$ and $P2Y_{12}$ cDNAs amplified from platelet mRNA by RT-PCR. A single nucleotide substitution (T → G) was identified within the translation initiation codon (ATG → AGG) in the patient's $P2Y_{12}$ cDNA (Fig. 4A). This substitution was also confirmed by reverse sequencing. No other nucleotide substitutions were detected within the coding region of either $P2Y_{12}$ or $P2Y_1$ cDNA from the patient. OSP-1 appeared homozygous for the substitution, and the substitution was not detected in 20 control subjects.

Nucleotide sequence analysis of PCR fragments from the patient's genomic DNA also suggested the homozygosity of the substitution (data not shown). To further confirm the homo-

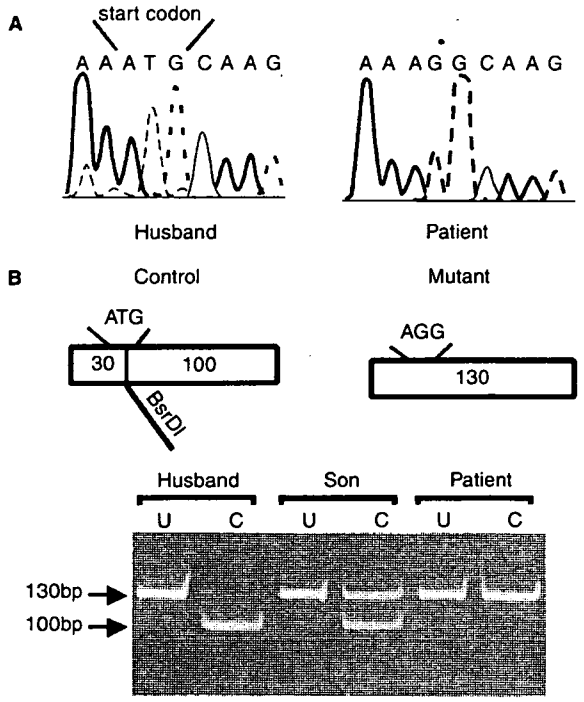

Fig. 4. Sequence analysis of $P2Y_{12}$ cDNA and restriction enzyme analysis of the $P2Y_{12}$ gene. (A) cDNA obtained by RT-PCR from platelet mRNA was analyzed by sequencing using a sense primer Y12F1. (B) PCR was performed to generate 130-bp fragments including initiation codon of $P2Y_{12}$ as described in Materials and methods. Undigested (U) or digested (C) PCR products with *Bsr*DI were analyzed on a 6% polyacrylamide gel. In patient OSP-1, the T → G mutation at position 2 abolishes a *Bsr*DI restriction site.

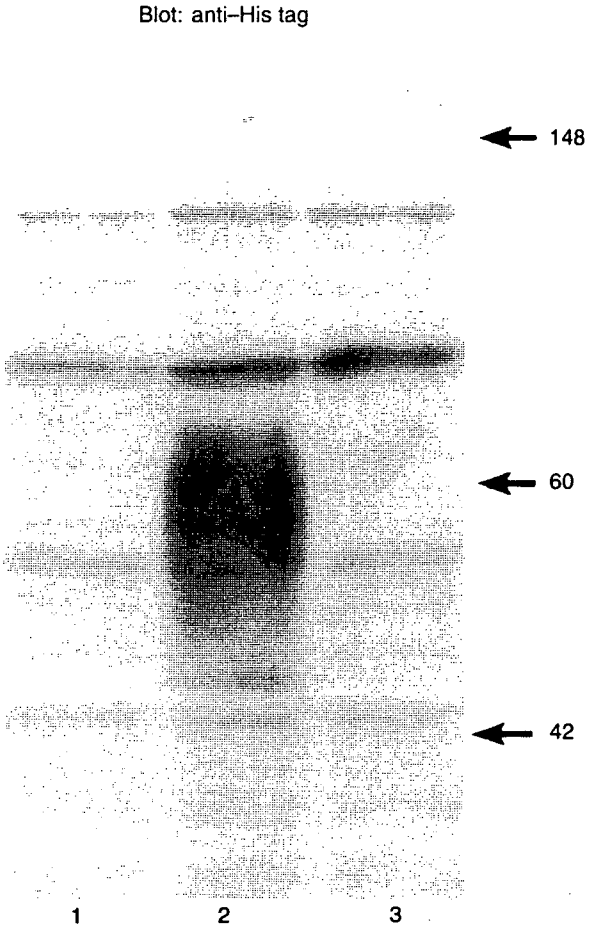

Fig. 5. Expression of $P2Y_{12}$ in HEK293 cells transfected with WT or mutant His-tag attached $P2Y_{12}$. Wild-type or mutant $P2Y_{12}$ construct was transfected into HEK293 cells using the calcium phosphate method. Transfectants were lyzed by 1% Triton X-100 PBS containing protease inhibitors 2 days after transfection. Cell lysates from mock transfectant (lane 1), cells transfected with WT $P2Y_{12}$ (lane 2) or mutant $P2Y_{12}$ (lane 3) were separated by 7.5% SDS-PAGE, and immunoblot was performed by anti-His-tag antibodies.

zygosity, allele-specific restriction enzyme analysis (ASRA) was performed. The region around the initiation codon of the $P2Y_{12}$ gene was amplified by PCR using primers *Bsr*DI-GF and Y12R4. A restriction site for *Bsr*DI would be abolished by the T → G substitution. As shown in Fig. 4B, ASRA clearly indicated that the patient and her son were homozygous and heterozygous for the substitution, respectively. These results also confirm that the substitution is inheritable.

Heterologous cell expression of WT and mutant $P2Y_{12}$

As the substitution at the translation initiation codon might induce an alternative translation starting at downstream ATGs leading to an expression of shorter form of $P2Y_{12}$, we decided to investigate effects of the substitution found in the patient on the expression of $P2Y_{12}$. Expression vectors encoding WT and mutant $P2Y_{12}$ in which His-tag was attached at the C-terminal portion of $P2Y_{12}$ were constructed as described in the Materials and methods. Wild-type or mutant $P2Y_{12}$ construct was transfected into HEK 293 cells, and then expressed proteins were analyzed 48 h after transfection in an immunoblot assay employing anti-His antibodies. As shown in Fig. 5, WT $P2Y_{12}$ protein with an apparent molecular weight of ~60 KDa was expressed in 293 cells as a His-tag-positive protein. In sharp contrast, the mutant $P2Y_{12}$-expression vector failed to express any His-tag-positive protein. These results provide strong evidence that the T → G substitution at the translation initiation codon of $P2Y_{12}$ cDNA is responsible for the $P2Y_{12}$ deficiency.

Platelet spreading on immobilized fibrinogen

As it has been well documented that release of endogenous ADP is required for full platelet spreading onto immobilized fibrinogen [23], we next analyzed the patient's platelet spreading in order to evaluate the role of $P2Y_{12}$. Control platelets adhered to fibrinogen underwent morphological changes ranging from filopodia protrusion to complete spreading, and 50.5% ± 21.3% of the adherent platelets spread (n = 3) (Fig. 6A). In sharp contrast, the patient's platelets showed an

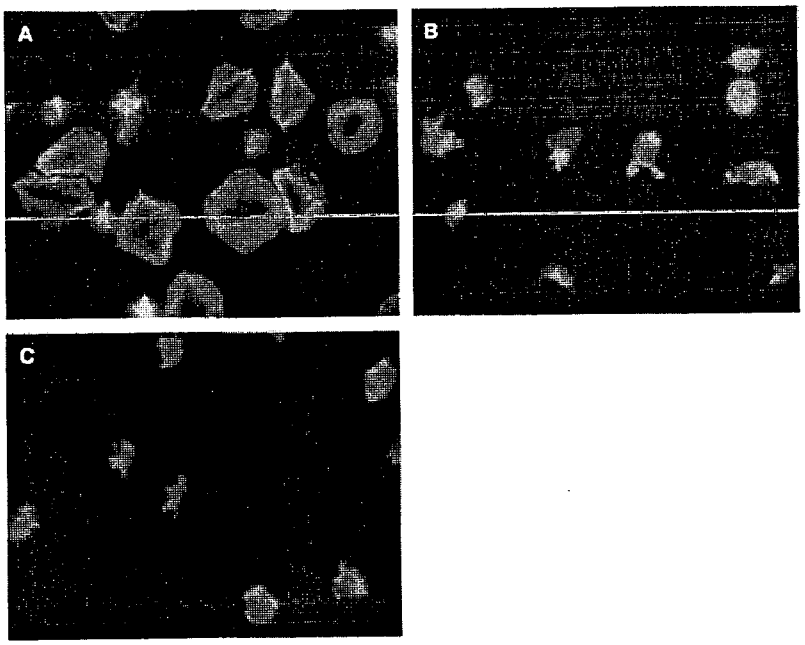

Fig. 6. Platelet spreading on immobilized fibrinogen. (A,B) Washed platelets from a control subject were applied onto fibrinogen-coated polystyrene dishes and incubated at 37 °C for 40 min without any inhibitor (A) or with 1 μM of AR-C69931MX (B). (C) Washed platelets from the patient were applied onto fibrinogen-coated polystyrene dishes and incubated at 37 °C for 40 min without any inhibitor. Adherent platelets were then fixed, permeabilized and stained with TRITC-conjugated phalloidin. Platelet morphology was analyzed by fluorescence microscopy.

impaired spreading and only 2.3% ± 1.4% of the adherent platelets spread ($n = 3$, $P < 0.001$, Fig. 6C). Similar results were obtained with control platelets in the presence of 1 μM of AR-C69931MX (6.2% ± 2.2%, $n = 3$, $P < 0.001$, Fig. 6B). In addition, 1 mM of A3P5P also markedly inhibited platelet spreading ($n = 3$, 10.1% ± 2.2%, $P < 0.001$, not shown). These results suggest that both $P2Y_{12}$ and $P2Y_1$ are necessary for platelet spreading.

Platelet-thrombus formation on immobilized collagen under flow conditions

To investigate the role of $P2Y_{12}$ in thrombus formation, we observed the real-time process of mural thrombogenesis on a type I collagen-coated surface under flow conditions with high shear rate (2000 s^{-1}) using the whole blood from OSP-1. Real-time observation revealed that thrombi formed on type I collagen were unstable. As platelet aggregates of the patient were loosely packed each other and unable to resist against high shear stress, most of the aggregates at the apex of the thrombi came off the thrombi constantly. On the other hand, most of thrombi formed by control platelets were densely packed with higher fluorescent intensity and were stable with constant growth during observation (Video 1 and 2).

As shown in Fig. 7A, the area covered with patient platelets after 7 min of flow was greater than that of control platelets (91.8% ± 0.3% vs. 82.2% ± 1.4%, $n = 3$, $P < 0.01$). However, thrombi formed by OSP-1 platelets were loosely packed, whereas thrombi were large and densely packed in controls. The overall fluorescent intensity of thrombi of OSP-1 platelets was lower than that of control platelets. Three-dimensional analysis revealed the striking difference in size and shape of individual thrombus formed after 10 min between the patient and control platelets (Fig. 7B). Thrombi formed by control platelets were large in size, clearly edged and surrounded by thrombus-free areas. On the other hand, individual thrombus formed by patient platelets was mostly small and appeared to be a thin layer of platelet aggregates. Thrombus height at the plateau phase was 10.2 ± 0.4 μm, which was less than half of controls (21.2 ± 0.4 μm).

Discussion

$P2Y_{12}$ coupled with $G\alpha_i$, primarily with $G\alpha_{i2}$, consists of 342 amino acid residues with seven transmembrane domains (TM), and its deficiency is responsible for congenital bleeding diathesis [10–16]. To date, five mutations responsible for a defect in the expression or the function of $P2Y_{12}$ in four different families have been demonstrated [10,15,16]. Patient ML possessed a mutation consisting of a two nucleotide deletion at amino acid 240 (near the N-terminal end of TM6), which would lead to a premature termination of $P2Y_{12}$ [10,14]. A two nucleotide deletions at amino acid 98 (next to the N-terminal end of TM3) and a single nucleotide deletion occurring just beyond TM3 were identified in other two families, both of which would lead to a premature termination of $P2Y_{12}$ [13,15]. However, in these reports expression studies had not been performed to show the direct association between these mutations and the $P2Y_{12}$ deficiency [10,15]. Patient AC, whose platelets expressed dysfunctional $P2Y_{12}$ with normal

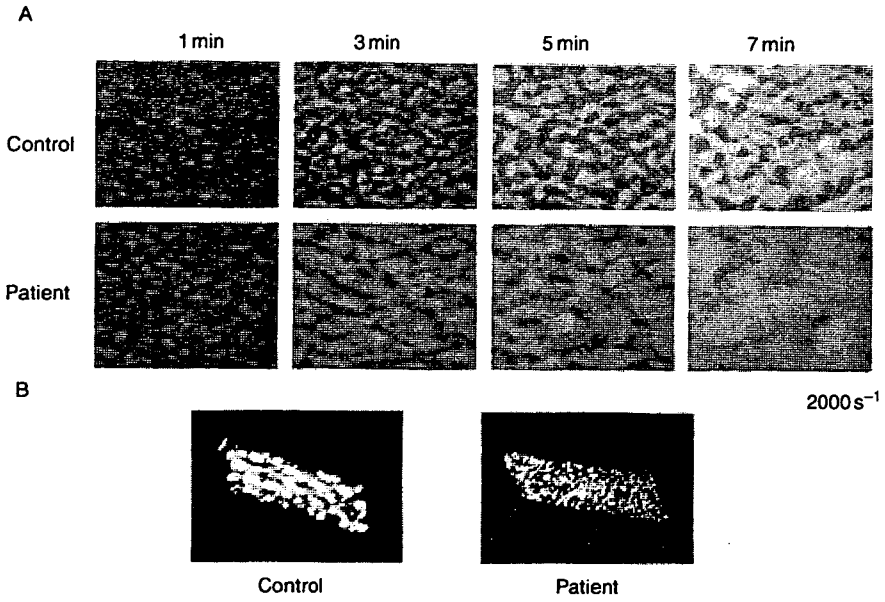

Fig. 7. Thrombus formation on immobilized collagen under flow conditions. (A) Whole blood containing mepacrine-labeled platelets obtained from the patient or control subjects was aspirated through a chamber with type I collagen-coated coverslips. Thrombi formed under a high shear rate (2000 s^{-1}) at indicated time points were observed using a microscope equipped with epifluorescent illumination and a CCD camera system. (B) Three-dimensional structure of thrombi formed after 10 min flow by platelets from the patient or a control subject was analyzed.

binding capacity of 2-methylthioadenosine 5′-diphosphate (2MeS-ADP), was compound heterozygous for Arg256 → Gln in TM6 and for Arg265 → Trp in the third extracellular loop of P2Y$_{12}$. Platelets from patient AC showed an increased platelet aggregation at high dose ADP compared with low dose ADP, suggesting the presence of residual receptor function [16]. In this study, we described a patient (OSP-1) with congenital bleeding diathesis bearing a novel homozygous mutation within the translation initiation codon (ATG → AGG) of the P2Y$_{12}$ gene. Consistent with previous studies, the aggregation of OSP-1 platelets with P2Y$_{12}$ deficiency was impaired to various agonists such as collagen, U46619, and PAR1 TRAP at low concentrations, but almost normal at high concentrations [11–14]. These findings confirmed the critical role of P2Y$_{12}$-mediated signaling evoked by endogenous ADP in platelet aggregation induced by low concentrations of agonists. In contrast to patient AC with residual P2Y$_{12}$-mediated signaling, the impaired platelet aggregation in OSP-1 in response to ADP was neither improved even at 100 μM of ADP stimulation nor reduced by adding 1 μM of AR-C69931MX, suggesting a complete loss of the P2Y$_{12}$ function. Family study confirmed that patient OSP-1 was homozygous for the mutation, and our expression study demonstrated that the mutation is responsible for the P2Y$_{12}$ deficiency.

A number of examples of mutations in the translation initiation codons have been demonstrated in various diseases [24]. Although some cases having mutations in the initiation codons did not express any related abnormal protein, Pattern *et al.* showed an abnormal Gα_s protein possibly synthesized as a result of initiation at downstream ATGs due to a mutation at an initiation codon (ATG → GTG) in patients with Albright's hereditary osteodystrophy [24,25]. In OSP-1, we detected the T → G mutation at position +2, and our expression study denied the possibility that the substitution might induce an alternative translation at downstream ATGs leading to an expression of shorter form of P2Y$_{12}$.

As to platelet spreading onto immobilized fibrinogen, OSP-1 platelets showed the impaired platelet spreading. Similarly, A3P5P inhibited the platelet spreading. It has been well documented that release of endogenous ADP is required for full platelet spreading onto immobilized fibrinogen [23], and Obergfell *et al.* [26] have demonstrated that the platelet spreading requires sequential activation of Src and Syk in proximately to $\alpha_{IIb}\beta_3$. In contrast to the ADP-induced platelet shape change shown in OSP-1 platelets in the platelet aggregometer, our data indicated that both P2Y$_{12}$ and P2Y$_1$ were necessary for the full spreading onto immobilized fibrinogen.

Employing clopidogrel or AR-C69931 MX as an inhibitor for P2Y$_{12}$, several studies examined the role of P2Y$_{12}$ in thrombogenesis under flow conditions [27–30]. However, some discrepancy between the studies was pointed out and non-specific effects of these inhibitors were not completely ruled out [28–30]. As patient OSP-1 was deficient in P2Y$_{12}$ as shown in this study, it would be informative to examine the real-time process of thrombogenesis on a type I collagen-coated surface under a high shear rate (2000 s^{-1}) employing whole blood obtained from OSP-1. Our data demonstrated that P2Y$_{12}$-deficiency led to the loosely packed thrombus and the impaired thrombus growth with enhancing adhesion to collagen, which was consistent with the study by Remijn *et al.* [30] employing patient ML's platelets. The increase in platelet adhesion to

collagen was probably due to the impaired platelet consumption by the growing thrombi [27,30]. Moreover, our real-time observation indicated that the loosely packed aggregates were unable to resist against high shear stress, and then most of the aggregates at the apex of the thrombi came off the thrombi. In contrast, Andre *et al.* [12] did not detect significant differences in *ex vivo* thrombus volume formed over human type III collagen under a shear rate of 871 s^{-1} between $P2Y_{12}^{-/-}$ and WT mice. Although Andre *et al.* used non-anticoagulated mouse blood instead of anticoagulated blood, Roald *et al.* [27] demonstrated that clopidogrel significantly reduced the thrombus volume over type III collagen employing non-anticoagulated human blood. Loosely packed platelet thrombi with swollen non-degranulated platelets were detected following clopidogrel intake, whereas densely packed thrombi with partly fused platelets were detected before clopidogrel intake by electron microscopy [27]. Thus, it is likely that differences between human and mouse, rather than those between non-anticoagulated and anticoagulated blood, may account for the discrepancy. Nevertheless, they showed that *ex vivo* thrombi were loosely packed and that only small and unstable thrombi were formed in $P2Y_{12}^{-/-}$ mice without reaching occlusive size in mesenteric artery injury model *in vivo* [12].

Our present study has demonstrated the novel mutation responsible for the $P2Y_{12}$ deficiency and suggested that secretion of endogenous ADP and subsequent $P2Y_{12}$-mediated signaling is critical for platelet aggregation, platelet spreading, and as a consequence, for stabilization of thrombus. Mild bleeding tendency observed in patient OSP-1 further emphasizes the efficacy of $P2Y_{12}$ receptor as a therapeutic target for thrombosis.

Acknowledgements

We thank Dr Mitsuhiko Sugimoto (Nara Medical University) for his valuable advice to perform the real-time observation of thrombogenesis under flow conditions. This study was supported in part by Grant-in Aid for Scientific Research from the Ministry of Education, Science and Culture in Japan, Grant-in Aid from the Ministry of Health, Labor and Welfare in Japan, Astellas Foundation for Research on Metabolic Disorder, Tukuba, Japan, and Mitsubishi Pharma Research Foundation, Osaka, Japan.

Supplementary material

The following supplementary material is available online at http://www.blackwell-synergy.com/loi/jth:

Figure S1. Perfusion study using control platelets. A real-time movie of platelets perfused over type-I collagen shows that thrombi formed by control platelets are densely packed and stable. This 5-second movie was taken at 5-minute perfusion under a high shear rate (2000 s^{-1}).

Figure S2. Perfusion study using OSP-1 platelets. A real-time movie of platelets perfused over type-I collagen shows that thrombi formed by the patient OSP-1 platelets are loosely packed and unstable. Newly formed aggregates on the top of thrombi keep on moving toward downstream and some aggregates came off the thrombi. This 5-second movie was taken at 5-minute perfusion under a high shear rate (2000 s^{-1}).

References

1 Fuster V, Badimon L, Badimon JJ, Chesebro JH. The pathogenesis of coronary artery disease and the acute coronary syndromes. *N Engl J Med* 1992; **326**: 242–50.

2 Antithrombotic Trialists' Collaboration. Collaborative meta-analysis of randomised trials of antiplatelet therapy for prevention of death, myocardial infarction, and stroke in high risk patients. *BMJ* 2002; **324**: 71–86.

3 Savage B, Almus-Jacobs F, Ruggeri ZM. Specific synergy of multiple substrate–receptor interactions in platelet thrombus formation under flow. *Cell* 1998; **94**: 657–66.

4 Tomiyama Y, Shiraga M, Shattil SJ. Platelet Membrane Proteins as Adhesion Receptors. In: Gresele P, Page C, Fuster V, Vermylen J, eds. *Platelets in thrombotic and non-thrombotic disorders pathophysiology, pharmacology and therapeutics*. Cambridge, UK: Cambridge, 2002: 80–92.

5 CAPRIE Steering Committee. A randomised, blinded, trial of clopidogrel versus aspirin in patients at risk of ischaemic events (CAPRIE). *Lancet* 1996; **348**: 1329–39.

6 Gachet C. ADP receptors of platelets and their inhibition. *Thromb Haemost* 2001; **86**: 222–32.

7 Dorsam RT, Kunapuli SP. Central role of the $P2Y_{12}$ receptor in platelet activation. *J Clin Invest* 2004; **113**: 340–5.

8 Fabre JE, Nguyen M, Latour A, Keifer JA, Audoly LP, Coffman TM, Koller BH. Decreased platelet aggregation, increased bleeding time and resistance to thromboembolism in $P2Y_1$-deficient mice. *Nat Med* 1999; **5**: 1199–202.

9 Leon C, Hechler B, Freund M, Eckly A, Vial C, Ohlmann P, Dierich A, LeMeur M, Cazenave JP, Gachet C. Defective platelet aggregation and increased resistance to thrombosis in purinergic $P2Y_1$ receptor-null mice. *J Clin Invest* 1999; **104**: 1731–7.

10 Hollopeter G, Jantzen HM, Vincent D, Li G, England L, Ramakrishnan V, Yang RB, Nurden A, Julius D, Conley PB. Identification of the platelet ADP receptor targeted by antithrombotic drugs. *Nature* 2001; **409**: 202–7.

11 Foster CJ, Prosser DM, Agans JM, Zhai Y, Smith MD, Lachowicz JE, Zhang FL, Gustafson E, Monsma Jr FJ, Wiekowski MT, Abbondanzo SJ, Cook DN, Bayne ML, Lira SA, Chintala MS. Molecular identification and characterization of the platelet ADP receptor targeted by thienopyridine antithrombotic drugs. *J Clin Invest* 2001; **107**: 1591–8.

12 Andre P, Delaney SM, LaRocca T, Vincent D, DeGuzman F, Jurek M, Koller B, Phillips DR, Conley PB. $P2Y_{12}$ regulates platelet adhesion/activation, thrombus growth, and thrombus stability in injured arteries. *J Clin Invest* 2003; **112**: 398–406.

13 Cattaneo M, Lecchi A, Randi AM, McGregor JL, Mannucci PM. Identification of a new congenital defect of platelet function characterized by severe impairment of platelet responses to adenosine diphosphate. *Blood* 1992; **80**: 2787–96.

14 Nurden P, Savi P, Heilmann E, Bihour C, Herbert JM, Maffran JP, Nurden A. An inherited bleeding disorder linked to a defective interaction between ADP and its receptor on platelets. Its influence on glycoprotein IIb-IIIa complex function. *J Clin Invest* 1995; **95**: 1612–22.

15 Conley P, Jurek M, Vincent D, Lecchi A, Cattaneo M. Unique mutations in the $P2Y_{12}$ locus of patients with previously described defects in ADP-dependent aggregation [abstract]. *Blood* 2001; **98**: 43b. Abstract 3778.

16 Cattaneo M, Zighetti ML, Lombardi R, Martinez C, Lecchi A, Conley PB, Ware J, Ruggeri ZM. Molecular bases of defective signal transduction in the platelet $P2Y_{12}$ receptor of a patient with congenital bleeding. *Proc Natl Acad Sci USA* 2003; **100**: 1978–83.
17 Shiraga M, Tomiyama Y, Honda S, Suzuki H, Kosugi S, Tadokoro S, Kanakura Y, Tanoue K, Kurata Y, Matsuzawa Y. Involvement of Na^+/Ca^{2+} exchanger in inside-out signaling through the platelet integrin $\alpha_{IIb}\beta_3$. *Blood* 1998; **92**: 3710–20.
18 Tomiyama Y, Tsubakio T, Piotrowicz RS, Kurata Y, Loftus JC, Kunicki TJ. The Arg-Gly-Asp (RGD) recognition site of platelet glycoprotein IIb-IIIa on nonactivated platelets is accessible to high-affinity macromolecules. *Blood* 1992; **79**: 2303–12.
19 Honda S, Tomiyama Y, Aoki T, Shiraga M, Kurata Y, Seki J, Matsuzawa Y. Association between ligand-induced conformational changes of integrin $\alpha_{IIb}\beta_3$ and $\alpha_{IIb}\beta_3$-mediated intracellular Ca^{2+} signaling. *Blood* 1998; **92**: 3675–83.
20 Kato H, Honda S, Yoshida H, Kashiwagi H, Shiraga M, Honma N, Kurata K, Tomiyama Y. SHPS-1 negatively regulates integrin $\alpha_{IIb}\beta_3$ function through CD47 without disturbing FAK phosphorylation. *J Thromb Haemost* 2005; **3**: 763–74.
21 Tsuji S, Sugimoto M, Miyata S, Kuwahara M, Kinoshita S, Yoshioka A. Real-time analysis of mural thrombus formation in various platelet aggregation disorders: distinct shear-dependent roles of platelet receptors and adhesive proteins under flow. *Blood* 1999; **94**: 968–75.
22 Honda S, Tomiyama Y, Shiraga M, Tadokoro S, Takamatsu J, Saito H, Kurata Y, Matsuzawa Y. A two-amino acid insertion in the Cys146-Cys167 loop of the α_{IIb} subunit is associated with a variant of Glanzmann thrombasthenia. Critical role of Asp163 in ligand binding. *J Clin Invest* 1998; **102**: 1183–92.
23 Haimovich B, Lipfert L, Brugge JS, Shattil SJ. Tyrosine phosphorylation and cytoskeletal reorganization in platelets are triggered by interaction of integrin receptors with their immobilized ligands. *J Biol Chem* 1993; **268**: 15868–77.
24 Cooper D. Human gene mutations affecting RNA processing and translation. *Ann Med* 1993; **25**: 11–7.
25 Patten J, Johns D, Valle D, Eil C, Gruppuso PA, Steele G, Smallwood PM, Levine MA. Mutation in the gene encoding the stimulatory G protein of adenylate cyclase in Albright's hereditary osteodystrophy. *N Engl J Med* 1990; **322**: 1412–9.
26 Obergfell A, Eto K, Mocsai A, Buensuceso C, Moores SL, Brugge JS, Lowell CA, Shattil SJ. Coordinate interactions of Csk, Src, and Syk kinases with αIIbβ3 initiate integrin signaling to the cytoskeleton. *J Cell Biol* 2002; **157**: 265–75.
27 Roald HE, Barstad RM, Kierulf P, Skjorten F, Dickinson JP, Kieffer G, Sakariassen KS. Clopidogrel - a platelet inhibitor which inhibits thrombogenesis in non-anticoagulated human blood independently of the blood flow conditions. *Thromb Haemost* 1994; **71**: 655–62.
28 Turner NA, Moake JL, McIntire LV. Blockade of adenosine diphosphate receptors $P2Y_{12}$ and $P2Y_1$ is required to inhibit platelet aggregation in whole blood under flow. *Blood* 2001; **98**: 3340–5.
29 Goto S, Tamura N, Handa S. Effects of adenosine 5′-diphosphate (ADP) receptor blockade on platelet aggregation under flow. *Blood* 2002; **99**: 4644–5.
30 Remijn JA, Wu YP, Jeninga EH, IJsseldiik MJ, van Willigen G, de Groot PG, Sixma JJ, Nurden AT, Nurden P. Role of ADP receptor $P2Y_{12}$ in platelet adhesion and thrombus formation in flowing blood. *Arterioscler Thromb Vasc Biol* 2002; **22**: 686–91.

Surgical Management of Distal Arch Aneurysm: Another Approach With Improved Results

Kenji Minatoya, MD, Hitoshi Ogino, MD, Hitoshi Matsuda, MD, Hiroaki Sasaki, MD, Toshikatsu Yagihara, MD, and Soichiro Kitamura, MD

Department of Cardiovascular Surgery, National Cardiovascular Center, Osaka, Japan

Background. Surgical treatment for distal arch aneurysm carries the risk of stroke. Although left thoracotomy has been used for repair of distal arch aneurysm as a standard approach, we have performed total arch replacement under deep hypothermia with circulatory arrest through a midsternotomy for this subset of aneurysms.

Methods. From January 1998 to February 2003, 119 patients underwent elective total arch replacement (mean age, 72.3 ± 6.0 years) for distal arch aneurysm under deep hypothermia with circulatory arrest. Antegrade selective cerebral perfusion was used for brain protection. Arch vessels were independently reconstructed using quadrifurcated grafts. Concomitant procedures included tricuspid annuloplasty in 1 patient, aortic valve operations in 2, sinotubular junction plication in 6, and coronary artery grafting in 22.

Results. The early mortality rate was 0.84% (1 of 119). The mean duration of circulatory arrest was 67.1 ± 19.7 minutes. Perioperative stroke rate was 0.84% (1 of 119). This stroke occurred 9 days postoperatively in an 81-year-old man with a history of cerebral infarction. Other complications were reexploration for bleeding in 1 patient (0.84%) and respiratory failure in 6 (5.0%).

Conclusions. This operative approach for distal arch aneurysm featured a low mortality rate and low risk of perioperative stroke. Concomitant cardiac surgery could be performed routinely in standard fashion. Distal arch aneurysms that do not involve a large segment of the descending thoracic aorta can thus be repaired with low mortality and few cerebral complications through a midsternotomy.

(Ann Thorac Surg 2006;81:1353–7)

Aneurysms that arise in the distal aortic arch and spare the innominate artery but not the left common carotid or subclavian artery can be approached through a standard left thoracotomy [1]. There is, however, a subset of distal arch aneurysms that do not involve a large segment of the descending thoracic aorta. This subset of aneurysms can be approached through midsternotomy. Although few reports are available concerning stroke after descending aortic surgery through left thoracotomy, stroke does indeed occur after surgery of the descending aorta, and is as frequent as for surgery of the ascending aorta [2]. We began to perform total arch replacement for distal arch aneurysms through a midsternotomy instead of replacement of diseased aorta through a left thoracotomy in our institution in the early 1990s, with a decrease in operative morbidity [3]. In this study, we evaluated recent surgical outcomes of total arch replacement for distal aortic arch aneurysm through a standard midsternotomy.

Accepted for publication Aug 25, 2005.

Presented at the Fortieth Annual Meeting of The Society of Thoracic Surgeons, San Antonio, TX, Jan 26–28, 2004.

Address correspondence to Dr Minatoya, Department of Cardiovascular Surgery, National Cardiovascular Center, 5-7-1 Fujishirodai, Suita, Osaka 565-8565, Japan; e-mail: minatoya@hsp.ncvc.go.jp.

Patients and Methods

Patients

From January 1998 to February 2003, 119 consecutive patients underwent elective total arch replacement for distal aortic arch aneurysm under deep hypothermia with circulatory arrest, and accounted for 64.3% of all patients (185) undergoing elective total arch replacement. Mean age was 72.3 ± 6.0 years, and there were 20 women. All patients underwent surgery on an elective basis. All aneurysms were atherosclerotic, and 50 patients (42%) had saccular type and 69 (58%) had fusiform type aneurysms.

Operative Techniques

The skin incision extended from the suprasternal notch to a point equidistant between the xiphoid process and umbilicus. To expose the left subclavian artery, a left hemicollar incision was added (Fig 1A). All operative maneuvers were performed through a midsternotomy.

The femoral artery or ascending aorta was used as a site of cannulation for arterial return. Ascending cannulation is preferable when atherosclerotic change in the ascending aorta is minimal on epiaortic echography. However, femoral arterial cannulation is used when the ascending aorta exhibits severe atherosclerotic change. Additional cannulation of the right axillary artery was employed in 97 cases (81.5%). Reperfusion and rewarming were always performed in antegrade fashion through

Published by Elsevier Inc

0003-4975/06/$32.00
doi:10.1016/j.athoracsur.2005.08.075

Ann Thorac Surg
2006;81:1353–7

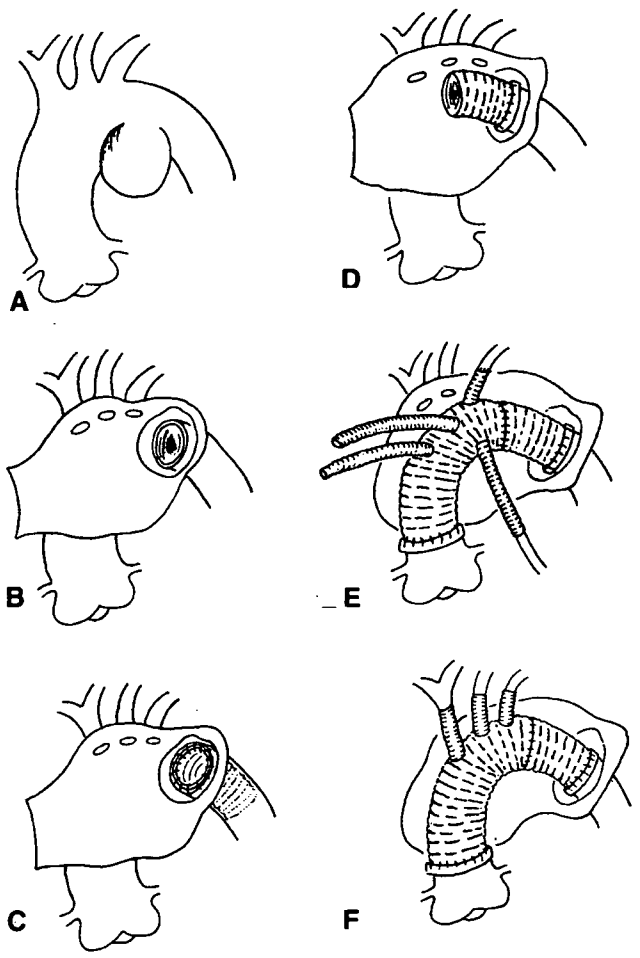

Fig 1. (A) The left subclavian artery. (B) Complete transaction of the descending aorta distal to the left subclavian artery. (C) A short graft was introduced into the lumen of the descending aorta, and then sewn to the aortic wall. (D) The short graft was pulled out of the descending aorta. (E) Quadrifurcated graft was anastomosed to the short graft, and then left subclavian artery was reconstructed. Proximal anastomosis to the ascending aorta was followed. (F) The left internal carotid artery, and the brachiocephalic artery were reconstructed.

the side branch of the quadrifurcated graft. For graft replacement, collagen woven or a gelatin-impregnated knitted Dacron (C. R. Bard, Haverhill, Pennsylvania) graft was used. Quadrifurcated graft was used for graft replacement. Arch vessels were independently reconstructed using the quadrifurcated graft, and the en-bloc repair technique was not used at all.

Open distal anastomosis was consistently performed with complete transaction of the descending aorta distal to the left subclavian artery (Fig 1B). The stepwise technique for distal anastomosis was employed in most cases. A short graft was introduced into the lumen of the descending aorta from the stump, and then sewn to the aortic wall with a running suture with 3-0 or 4-0 polypropylene (Fig 1C). The short graft was then pulled out of the descending aorta (Fig 1D). At the suture line, the graft was inverted circumferentially and fixed to the aortic wall properly. In rare cases, bleeding is observed from this suture line, but hemostasis is easily achieved with an additional stitch. Finally, quadrifurcated graft was anastomosed to the short graft with running sutures of 2-0 or 3-0 polypropylene (Fig 1E). That was followed by anastomosis of the left subclavian artery, proximal anastomosis to the ascending aorta, the left internal carotid artery, and final anastomosis of the brachiocephalic artery (Fig 1F).

Antegrade cerebral perfusion was performed with an ordinary arterial cannula in the right axillary artery, or with a balloon-tip cannula inserted directly into the brachiocephalic artery from inside the aortic arch, and in the left common carotid artery. The left subclavian artery was usually clamped, except in patients with a dominant left vertebral artery. Cerebral perfusion flow was maintained at 300 to 500 mL/min; the mean pressure in the superficial temporal arteries ranged from 40 to 60 mm Hg, and the nasopharyngeal temperature ranged from 20° to 26°C. We have, since 1997, gradually elevated hypothermc circulatory arrest temperature from 20° to 26°C for aortic arch surgery. Monitoring of perfusion pressure bilaterally in the superficial temporal arteries was performed using standard methods. Neurologic monitoring, including electroencephalography, was not performed during surgery.

Concomitant Procedures

Concomitant procedures included tricuspid annuloplasty in 1 patient, aortic valve operations in 2, sinotubular junction plication in 6, and coronary artery grafting in 22. These procedures could be performed routinely in standard fashion through a midsternotomy.

Results

The mean duration of circulatory arrest was 67.1 ± 19.7 minutes. A second pump run after weaning from cardiopulmonary bypass was required in 4 patients because of bleeding at the distal anastomosis. In these cases, hemostasis was accomplished through midsternotomy without an additional incision for left thoracotomy. The early mortality rate was 0.84% (1 of 119). This patient was a 72-year-old man with a history of myocardial infarction, and the reason for death was low output syndrome due to perioperative myocardial infarction. Perioperative stroke rate was 0.84% (1 of 119). This stroke occurred 9 days postoperatively in an 81-year-old man with a history of cerebral infarction. He had exhibited atrial fibrillation postoperatively, and atrial fibrillation was thought to have been the reason for the stroke. Seven patients (5.9%) had transient neurologic deficit, and 4 (3.4%) had hoarseness. Other complications were reexploration for bleeding in 1 patient (0.84%) and respiratory failure in 6 (5.0%). All patients who survived surgery underwent postoperative computed tomography, which revealed no problems with grafts including branches for arch vessels.

Comment

Distal arch aneurysms have been considered a subset of aneurysms of the descending thoracic aorta. Left thoracotomy has therefore been used as a standard approach for replacement of the diseased segment in patients with them. However, the distal arch can also be approached through a midsternotomy.

Stroke is a devastating complication of aortic surgery. The occurrence of it after descending aorta surgery seems somewhat counterintuitive, as the descending aorta, which is downstream from the head vessels, might not be expected to be a significant source of air or particulate matter [2]. Surgical treatment for distal aortic arch aneurysm through left thoracotomy does, however, carry the risk of stroke. Although reports on the risk of stroke after descending thoracic aneurysm repair are limited, some [4, 5] have indicated that it is 3.3% to 8.1%. Manipulation of the aortic arch for proximal control in descending aortic operations is thought to be one factor predisposing to stroke. The proximal clamp must be placed close to the subclavian artery with or without bypass or shunt in most strategies for descending aortic repair [6].

Surgery of the aortic arch also features the risk of stroke. It is usually performed under deep hypothermic circulatory arrest with or without cerebral perfusion. Techniques for brain protection have gradually improved in the last 10 years, and the rate of stroke has significantly decreased [7, 8]. Another factor possibly reducing neurologic complications is right axillary artery perfusion. Since we began using this type of perfusion, the rate of stroke in our patients has dramatically decreased. The antegradely perfused aortic flow through the axillary artery conflicts with retrogradely perfused femoral artery flow in the descending aorta. Cerebral embolism caused by retrograde femoral artery perfusion or direct insertion of a perfusion cannula from atheromatous brachiocephalic artery can be prevented with axillary artery perfusion [9]. However, because the size of the artery was only enough for cannulas of 12F to 16F in size, this axillary perfusion could not sustain total body perfusion. In the present series, the rate of stroke was only 0.8%, and the one stroke that occurred was thought to be due to postoperative atrial fibrillation. This is the lowest incidence of stroke among reports on the repair of distal arch aneurysm [10].

During the same period in our institution, 81 consecutive patients underwent descending aortic aneurysm repair under partial cardiopulmonary bypass through a left thoracotomy and 24 consecutive patients underwent descending aortic aneurysm repair under deep hypothermic circulatory arrest through a left thoracotomy. Although no paraplegia developed in either group, 2 patients (2.5%) in the former group and 3 patients (12.5%) in the latter group suffered stroke postoperatively. In fact, the rate of stroke was lower in our group, for which meticulous brain protection technique was used, than in these other groups of patients.

Distal anastomosis to the descending aorta should be performed within a limited period under hypothermic circulatory arrest. Technically, the distal anastomosis is the most strenuous part of total arch replacement performed through a midsternotomy. The suture line is sometimes quite deep from the midline, and it is difficult to place an additional stitch for hemostasis. Therefore, the anastomosis should be secured and safely performed within a limited amount of time. There have been several reports on alternative methods of exposure of the distal aortic arch for surgical intervention [11–13]. These alternatives have been introduced for distal anastomosis, which is usually difficult, especially in patients with diseased descending aorta. These approaches generally require longer incisions and cannot be considered less invasive. Another alternative is stent grafting. Sueda and colleagues [14] report that transaortic endovascular stent grafting was an effective alternative approach for distal arch aneurysm. For unclear reasons, however, it features the risk of paraplegia. Moreover, long-term follow-up data have not yet been reported for it.

Complete transection of the descending aorta for open distal anastomosis is important for preventing injury of the left recurrent nerve. We believe that the inclusion technique of anastomosis carries the risk of left recurrent nerve injury, and that complete dissection of the stump is of key importance in avoiding such injury. In this series, only 4 patients had mild hoarseness, but no serious recurrent nerve palsy followed.

We have used the stepwise technique routinely for distal anastomosis for the reasons noted above. Though the anastomosis requires an additional 10 to 15 minutes, performance of it is much easier than direct suturing even with limited exposure, and features less risk of bleeding. With this stepwise technique, no additional incision is needed for exposure, unless repair of a longer segment of the descending aorta is necessary. Only when the anastomosis is difficult with the use of this stepwise technique should an additional left thoracotomy be considered. In this series, additional left thoracotomy was not required, even though some patients required another pump run for hemostasis. The difficulty of anastomosis was appropriately evaluated preoperatively by computed tomography or magnetic resonance imaging. When the aneurysm does not extend beyond the level of the left pulmonary artery, distal anastomosis of the graft can, in our experience, be performed through a midsternotomy.

It might still be questioned whether total arch replacement for distal arch aneurysm is excessive, since the transverse arch and a part of the ascending aorta, which are not diseased, are also replaced. We believe, however, that there are several advantages to complete total arch replacement for patients with distal arch aneurysm. First, the risk of embolization as a cause of neurologic deficits can be reduced. Many patients with distal arch aneurysm have severe atherosclerotic change in the thoracic aorta, which is often widespread. We often encounter severe atherosclerotic change at the origin of the arch vessels in patients with distal arch aneurysm. Thus, the ascending and transverse aorta are, in addition to the diseased